International Conference on Applied Energy 2019
Aug 12-15, 2019, Västerås, Sweden
Paper ID: 268

PERFORMANCE INVESTIGATION OF PARALLEL-PLATE BASED THERMOELECTRIC GENERATOR WITH DIFFERENT THERMOELECTRIC MODULE LAYOUTS

Ruochen Wang[1*], Zihan Meng [2], Ding Luo [2], Wei Yu [2]

1 *Automotive Engineering Research Institute, Jiangsu University, Zhenjiang 212001, China*

2 *School of Automotive and Traffic Engineering, Jiangsu University, Zhenjiang 212001, China*

ABSTRACT

Thermoelectric generators (TEGs) have been widely used to recover high temperature waste gas in recent years. The TEG performance relates directly to the hot side temperature of thermoelectric modules (TEMs) which is highly affected by the layouts of modules. By the numerical results, it is found that the structure of TEMs uniformly distributed on the four sides of the heat exchanger can reach the smallest temperature difference at the air temperature of 500K and air velocity of 2.4m/s. Also, the TEMs distributed on the one side of the heat exchanger can achieve the highest output power of 11.36W whereas the highest efficiency is reached for the structure of TEMs uniformly distributed on the four sides of the heat exchanger. It can be concluded that the higher coverage ratio of TEMs on the surfaces of heat exchanger is, the higher conversion efficiency may bring. The findings of this work may provide a new method to improve the performance of TEG.

Keywords: thermoelectric modules, heat exchanger, output power, efficiency, coverage ratio

1. INTRODUCTION

Energy is the basis for the survival and development of human society. With the development of industrial civilization, the use of fuel is causing a great number of energy and environmental problems. As a solid-state energy converter, thermoelectric generator (TEG) can directly convert the collected waste heat into electricity with the advantages of saving fuel consumption and no environmental-harmful emissions. Nowadays, TEGs are widely used in different fields, including electricity generation in extreme environments, waste heat recovery in ships, automobile, industries, domestic thermoelectric generation systems and solar thermoelectric generator [1]. Since TEG has the shortcoming of low heat-to-electricity conversion efficiency, many researchers devoted themselves to enhancing the efficiency of TEG.

Some previous researches focused on the structure of TEG and the layout of Thermoelectric modules (TEMs). Huang et al. [2] presented a novel design of a concentric cylindrical thermoelectric generator (CCTEG) and an annular thermoelectric module (ATEM). Their results indicate that the open circuit electric potential of the ATEM is more than that of the traditional TEM. Shittu et al. [3] proposed a segmented annular thermoelectric generator (SATEG) with round shaped heat sink to eliminate the thermal contact resistance, and the results show that the efficiency of the SATEG is greater than that of the Bismuth telluride annular thermoelectric generator (ATEG) and Skutterudite ATEG. Borcuch et al. [4] considered the influence factors of a hexagonal heat exchanger (HHX) with six different fin geometries, and they found that HHX can produce 350W net electric power with the equal fins on both sides of the heat exchanger. André et al. [5] carried out a numerical simulation on three different heat exchanger configurations with plain, offset strip or triangular fins. It is demonstrated that the thickness of the fins, the exhaust pipes, the cooling pipe walls, the electrical conductor and the ceramic strips should be controlled to reduce the effect of this thickness on the net power.

Numerical simulation has been developed as a powerful tool to work out the output power and conversion efficiency of the TEG. He et al. [6] established an advanced numerical model of multi-element thermoelectric components in series and studied the thermoelectric performance under four cooling modes. The consequences reveal that the power produced by counterflow mode is obviously higher than that produced by coflow mode under air cooling. Meng et al. [7] developed a multi-physical, steady-state, and three-dimensional numerical model to investigate the TEG performance. The results indicate that the output power elevate slightly, but the conversion efficiency decreases markedly when heat losses exist between TEG and the ambient. Du et al. [8] conducted numerical analysis to discuss the impact of Tomson effect on one-stage thermoelectric cooler (TEC), and they found that bigger current, higher temperature of hot side, or lower heat load all can increase the temperature difference between the cold and hot sides.

As mentioned above, there are a number of techniques to elevate the output power and conversion efficiency of TEG. In this paper, the influence of the TEM layouts on the TEG performance is studied via a numerical model. The investigations of temperature distributions, output power and conversion efficiency on the structures with five TEM layouts are conducted. The findings of this work may guide the design of heat exchanger when pursuing the maximum power or maximum efficiency.

2. NUMERICAL MODEL

2.1 The model of fluid flow

Equations for the conservation of mass, momentum, and energy for the fluids in the flow channel of heat exchanger are:

$$\nabla \cdot v = 0 \tag{1}$$

$$\nabla \cdot (vv) v = -\frac{1}{\rho} \nabla p + \nabla \cdot (\mu \nabla v) \tag{2}$$

$$\nabla \cdot \left(\lambda \nabla T \right) = \rho c v \cdot \nabla T \tag{3}$$

In Eq. (3), v , c , ρ and μ are the velocity, specific heat capacity, the density and the kinetic viscosity of the fluids respectively, and λ is the material thermal conductivity.

The fluid flow herein presents the pattern of turbulent flow, and the renormalization group (RNG) $k-\varepsilon$ turbulence model is adopted due to its higher adaptivity and accuracy. More details of the RNG $k-\varepsilon$ turbulence model can be found in Ref. [9].

2.2 Main equations for the modeling of thermoelectric module

The steady-state energy conservation equations in p-type and n-type semiconductors are:

$$\nabla \cdot (\lambda_{\mathrm{P}}(T) \nabla T_{\mathrm{P}}) = -\frac{1}{\sigma_{\mathrm{P}}}(T) J^2 + \nabla \alpha_{\mathrm{P}}(T) J T_{\mathrm{P}} \tag{4}$$

$$\nabla \cdot (\lambda_{\mathrm{N}}(T) \nabla T_{\mathrm{N}}) = -\frac{1}{\sigma_{\mathrm{N}}}(T) J^2 + \nabla \alpha_{\mathrm{N}}(T) J T_{\mathrm{N}} \tag{5}$$

In Eq. (4) and Eq. (5), $\frac{1}{\sigma_{\mathrm{P,\,N}}}$, $\lambda_{\mathrm{P,\,N}}$ and $\alpha_{\mathrm{P,\,N}}$ are the electric resistivity, thermal conductivity and Seebeck coefficient of p-type and n-type semiconductors, respectively. J is the current density vector.

For the copper electrodes, its energy conservation equation can be expressed as:

$$\nabla \cdot \left(\lambda_{\mathrm{co}} \nabla T \right) = -\frac{1}{\sigma_{\mathrm{co}}} J^2 \tag{6}$$

where $\frac{1}{\sigma_{\mathrm{co}}}$ and λ_{co} are electric resistivity and thermal conductivity of the copper electrodes respectively.

The electric field intensity vector along the thermoelectric materials can be defined by:

$$E = -\nabla \phi + \alpha \nabla T \tag{7}$$

where ϕ is the electric potential, and $\alpha \nabla T$ is the Seebeck voltage.

The current density vector in Eqs. (4) – (6) can be written as:

$$J = \sigma E \tag{8}$$

Otherwise, the continuity of current in the semiconductors and copper electrodes can be expressed as:

$$\nabla J = 0 \tag{9}$$

2.3 Boundary conditions

The thermoelectric module is the core part of TEG, its high-temperature surface is in close contact with heat exchanger, while the temperature of the cold side is fixed at 300K. Besides, the ambient convective heat transfer boundary condition is defined as follows:

$$-\lambda \frac{\partial T}{\partial n} = h_{\mathrm{a}} \left(T - T_{\mathrm{a}} \right) \tag{10}$$

where, $h_{\mathrm{a}} = 10\mathrm{W/(m^2 \cdot} K)$ is ambient convective coefficient and $T_{\mathrm{a}} = 293K$ is ambient temperature respectively.

At the inlet and outlet of flow channels, the boundary conditions of velocity inlet and pressure outlet are defined, and the inlet velocity and inlet air temperature are 2.4m/s and 500K respectively for all five cases. The outlet pressure is set to be equal a standard atmospheric pressure. One of the terminals of each TEM is grounded.

Besides, the internal resistance of each TEM can be computed by:

$$R_{\mathrm{tem}} = N \left(\frac{L_{\mathrm{P}}}{\sigma_{\mathrm{P}} A_{\mathrm{P}}} + \frac{L_{\mathrm{N}}}{\sigma_{\mathrm{N}} A_{\mathrm{N}}} \right) \tag{11}$$

where, *N* means the number of the thermocouples in a thermoelectric module, $A_{\mathrm{P,N}}$ and $L_{\mathrm{P,N}}$ are cross-sectional area and length of a p-type and an n-type semiconductor.

Thus, conversion efficiency of TEG can be defined as:

$$\eta = \frac{\sum \frac{V^2}{R_{\mathrm{tem}}}}{c\dot{m}\left(T_{\mathrm{in}} - \mathrm{T}_{\mathrm{out}}\right)} \tag{12}$$

where, *V* is the open circuit electric potential of each TEM, $\dot{m}$ is mass flow rate of the air, T_{in} and T_{out} are the temperature of the inlet and outlet respectively.

3. THE STRUCTURE OF TEG

All the geometries of the TEGs regarding the layout of TEMs were drawn in CATIA software and they were individually imported to COMSOL for the numerical simulations.

3.1 Five TEG structures

The described TEGs with different layouts of TEMs are as shown in Fig 1. The TEGs consist of three main components, including inlet and outlet connectors, heat exchanger and thermoelectric modules. The width and height of the heat exchanger are the same for the purpose of preventing the effect of sizes on the TEG performance. In order to simplify the simulation process, the cooling water tank is not set at the cold side of TEMs in the three-dimensional structure. A fixed temperature can be directly added to the cold side of the TEMs.

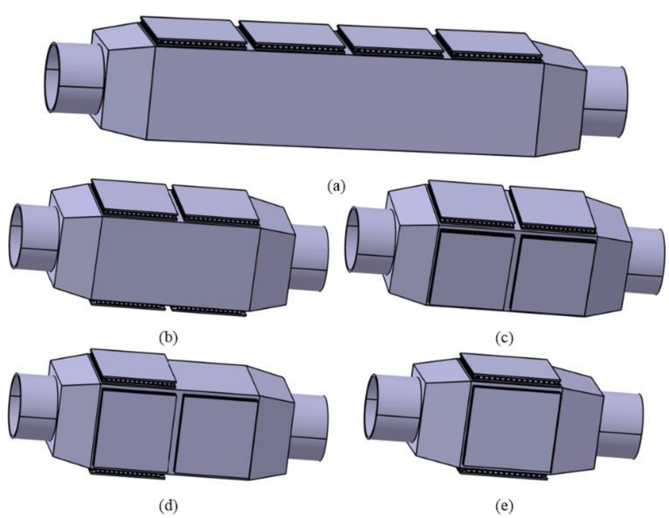

Fig 1 Three-dimensional TEG structure with different TEMs layout

Fig 1 (a) shows that four TEMs are arranged on the same side of heat exchanger. Fig 1 (b) and (c) indicate that TEMs are divided into twosome where the two TEM groups are placed on the opposite sides in Fig 1 (b) but the two groups of TEMs are placed on the adjacent sides in Fig 1 (c). Fig 1 (d) shows TEMs are separate into three groups and are placed on three sides of heat exchanger. Fig 1 (e) reveals that TEMs are arranged on four sides of heat exchanger to take full advantage of the heat from each side.

3.2 Dimensional and material parameters of TEM

As shown in Fig 2, TEM consists of a series of thermocouples, each of which is made up of a p-type (colored in red) and an n-type (colored in blue) semiconductor connected with copper sheet (colored in grey), and all of the thermoelements and copper electrodes are sandwiched between two ceramic plates (colored in khaki). The parameters of the TEM in this paper are shown in Table 1.

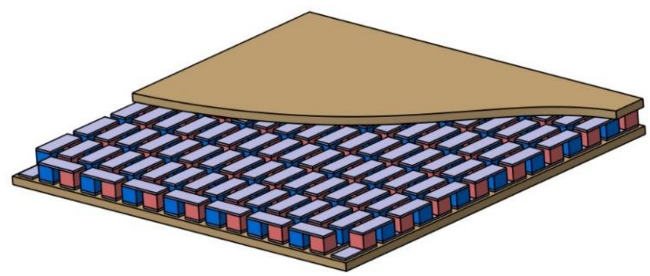

Fig 2 Three-dimensional structure of the thermoelectric module

Thermocouples should have high electrical conductivity and low thermal conductivity to achieve a better TEG performance. In this paper, Bismuth Telluride (Bi_2Te_3) was chosen as the material for the thermocouples. Bi_2Te_3 is basically known as an efficient thermoelectric material at low temperature.

4. RESULTS AND DISCUSSION

4.1 Temperature analysis of TEG with different TEM layouts

Fig 3 shows the temperature distributions of five structures at the inlet temperature of 500K, the fixed cold side temperature of 300K and the air velocity of 2.4m/s. It is obvious that the temperature difference between the inlet and the outlet of the structure (a) is the largest, which is about 134K. The smallest temperature difference between the inlet and the outlet is around 60K from the structure (e). It can be concluded that the similar temperature difference of the other three structures is approximately 95K. These comparisons explain that the ambient convective heat transfer plays a great influence on temperature changes.

Table 1 Parameters of TEM

Parameters	P	N	Copper	Ceramic
Number	127	127	255	2
Height(mm)	1.4	1.4	0.2	0.8
Length·width(mm^2)	1.7•1.7	1.7•1.7	1.7•4.2	40•40
Seebeck coefficient (μV/ K)	$-7.71\cdot10^{-10}T^2$ $+8.05\cdot10^{-7}T$ $+3.82$	$7.71\cdot10^{-10}T^2$ $-8.05\cdot10^{-7}T$ -3.82	-	-
Thermal conductivity ($W\cdot m^{-1}\cdot K^{-1}$)	$4.57\cdot10^{-5}T^2$ $-0.03T+6.70$	$4.57\cdot10^{-5}T^2$ $-0.03T+6.70$	400	175
Electrical resistivity ($10^5\Omega\cdot m$)	$1.34\cdot10^{-5}T^2$ $-1.22\cdot10^{-3}T$ $+3.33$	$1.34\cdot10^{-5}T^2$ $-1.22\cdot10^{-3}T$ $+3.33$	$5.998\cdot10^{-7}$	-

This difference means that the total heat absorption is not the same. The different values of the temperature variation lead to different hot side temperature of TEMs by heat exchanger, which significantly affects the open circuit electric potential of TEM because Seebeck voltage is proportional to the temperature difference on both sides of TEM.

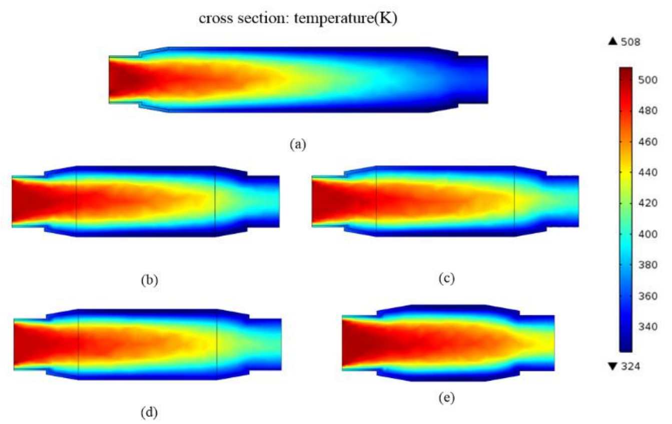

Fig. 3 Temperature variation of heat exchanger

4.2 Electric potential analysis of TEG with different TEM layouts

Fig 4 shows the three-dimensional electric potential distributions about different structures. Different colors indicate different electric potential. Fig 4 (a) indicates the electric potential of TEMs which are arranged on one side of the heat exchanger. One of TEMs is magnified in order to clarify the electric potential. It is observed that the maximum open circuit electric potential and the minimum one are 2.72V and 1.43V respectively in Fig 4 (a) and (e) according to the legend. The thermal energy is only provided for one side in Fig 4 (a), but the heat is exchanged with four sides of the heat exchanger in Fig 4 (e). The open circuit electric potential generated by a single TEM decreases along with the direction of hot fluid flow because of the gradual decrease of the temperature difference between the two sides of TEM.

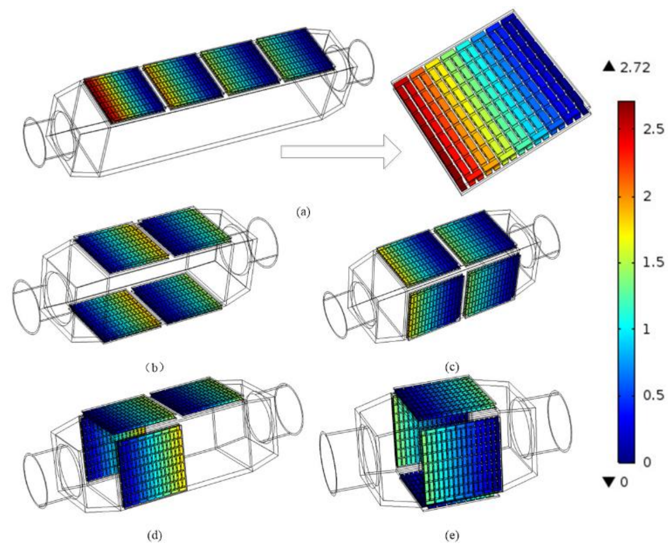

Fig 4 Electric potential comparison of TEMs

Fig 4 (b) and (c) show the different layouts on the two sides of the heat exchanger, which generate a similar electric potential. But the total voltage generated by TEMs in Fig 4 (b) is about 0.3V which is slightly higher than that in Fig 4 (c). It illustrates that the thermal energy can be utilized to a great extent in structure (b). However, the other two sides in structure (c) dissipate more heat to the ambient compared to structure (b).

Fig 5 reveals the comparison of power and heat utilization efficiency for five TEG structures. The structure (a) has the largest total power of 11.36W because it absorbs more heat while it has the smallest efficiency of 1.78% compared with other structures. And structure (e) has the minimum total power of 5.51W whereas its efficiency can reach the highest value of 2.26% among five structures. In general, the power decreases and the heat-to-electricity conversion efficiency increases from structure (a) to structure (e). Since the coverage ratio of TEMs on the surfaces of heat exchanger is the highest in structure (e), causing the be less heat transfer between the heat exchanger and the ambient. Consequently, the higher coverage ratio of TEMs on the surfaces of heat exchanger is, the higher conversion efficiency of TEG may get.

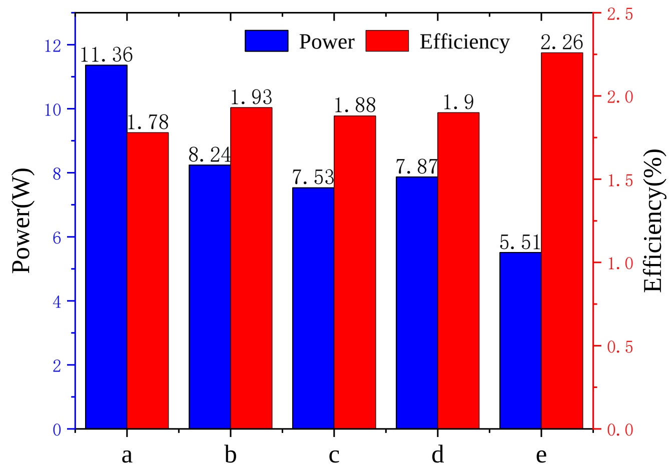

Fig 5 The comparison of power and conversion efficiency for five TEG structures

5. CONCLUSIONS

This paper presented five TEG structures with different TEM layouts on the surfaces of heat exchanger. The investigations of temperature distributions, output power and conversion efficiency are conducted. The performance evaluation of five TEG structures were concluded via the comparison of performance of five TEG structures. Based on the finds above, the following conclusions can be reached:

(1) The temperature of the structure with TEMs arranged on the same side of heat exchanger drops fastest at the air temperature of 500K and air velocity of 2.4m/s, which is approximately 134K. Nevertheless, the structure of TEMs uniformly distributed on the four sides of the heat exchanger can reach the smallest temperature difference of 60K.

(2) The TEMs distributed on the one side of the heat exchanger can achieve the highest output power of 11.36W whereas the highest efficiency of 2.26% is reached for the structure of TEMs uniformly distributed on four sides of the heat exchanger. It seems that the conversion efficiency of TEG increases with the coverage ratio of TEMs on the surfaces of heat exchanger.

REFERENCE

[1] Champier Daniel. Thermoelectric generators: A review of applications. Energy Convers Manage 140 (2017) 167–181.

[2] Kuo Huang, Bo Li, Yuying Yan, Yong Li, Ssennoga Twaha, Jie Zhu. A comprehensive study on a novel concentric cylindrical thermoelectric power generation system. Appl Therm Eng 117 (2017) 501–510.

[3] Samson Shittua, Guiqiang Lia, Xudong Zhaoa, Xiaoli Maa, Yousef Golizadeh Akhlaghia, Emmanuel Ayodele. High performance and thermal stress analysis of a segmented annular thermoelectric generator. Energy Convers Manage 184 (2019) 180–193.

[4] Marcin Borcuch, Michał Musiał, Stanisław Gumuła, Karol Sztekler, Krzysztof Wojciechowski. Analysis of the fins geometry of a heat exchanger on the performance parameters of a thermoelectric generation system. Appl Therm Eng 127 (2017) 1355–1363.

[5] André Marvão, Pedro J. Coelho, Helder C. Rodrigues. Optimization of a thermoelectric generator for heavy-duty vehicles. Energy Convers Manage 179 (2019) 178–191.

[6] Wei He, Shixue Wang, Chi Lu, Xing Zhang, Yanzhe Li. Influence of different cooling methods on thermoelectric performance of an engine exhaust gas waste heat recovery system. Appl Energy 162 (2016) 1251–1258.

[7] Jinghui Meng, Xinxin Zhang, Xiaodong Wang. Characteristics analysis and parametric study of a thermoelectric generator by considering variable material properties and heat losses. Int J Heat Mass Transfer 80 (2015) 227–235.

[8] Chienyi Du, Changda Wen. Experimental investigation and numerical analysis for one-stage thermoelectric cooler considering Thomson effect. Int J Heat Mass Transfer 54 (2011) 4875–4884.

[9] Ding Luo, Ruochen Wang, Wei Yu, Weiqi Zhou. Performance evaluation of a novel thermoelectric module with BiSbTeSebased material. Appl Energy 238 (2019) 1299–1311.